ISSN 1666-6070

MECÁNICA COMPUTACIONAL

Vol. XXXI

Alberto Cardona
Paul H. Kohan
Ricardo D. Quinteros
Mario A. Storti
(Eds.)

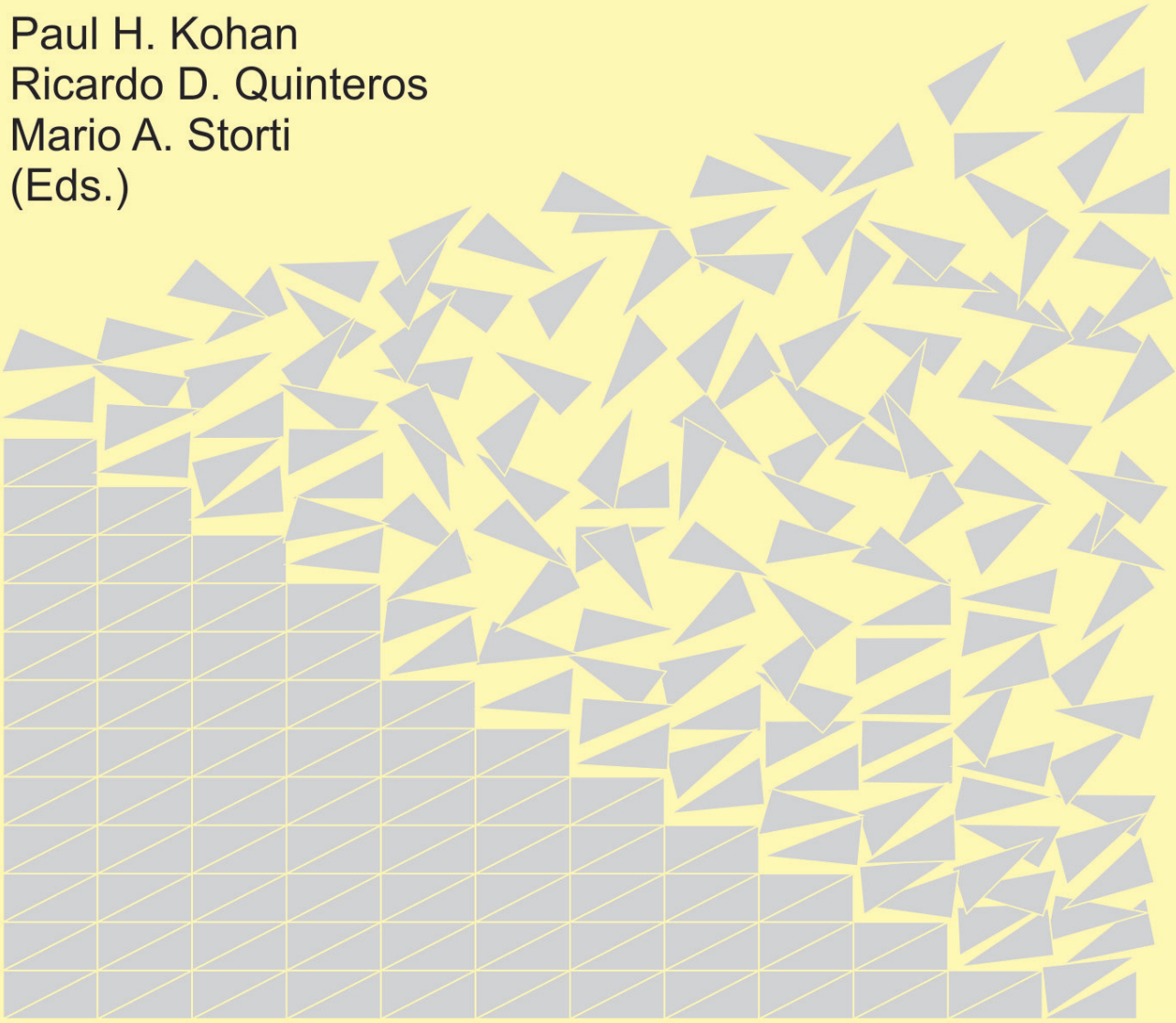

Asociación Argentina de
Mecánica Computacional

Asociación Argentina
de Mecánica Computacional

Mecánica Computacional Vol XXXI, págs. 1571-1590 (artículo completo)
Alberto Cardona, Paul H. Kohan, Ricardo D. Quinteros, Mario A. Storti (Eds.)
Salta, Argentina, 13-16 Noviembre 2012

MODELLING VISCOELASTIC BEHAVIOUR OF CARBON NANOTUBE-REINFORCED THERMO-PLASTICS

F. Otero[a,b], S. Oller[a,b], X. Martínez[b,c] and O. Salomón[b]

[a]*Departamento de Resistencia de Materiales y Estructuras en la Ingeniería, ETSECCPB, Universidad Politécnica de Cataluña, Barcelona, España.*

[b]*Centro Internacional de Métodos Numéricos en Ingeniería (CIMNE), Barcelona, España.*

[c]*Departamento de Ciencia e Ingeniería Náutica, FNB, Universidad Politécnica de Cataluña, Barcelona, España.*

Keywords: Carbon nanotubes, Composites, FEM, Constitutive model.

Abstract. Carbon nanotubes (CNTs), since their discovery by Lijima (S. Lijima, *Nature*, 354:56-58 (1991)), are considered a new generation of reinforcement. Their "nano" size structure makes them potentially free of defects, which provides them with excellent physical properties. There are two main nanotube types: single wall nanotubes (SWCNTs), which are made of a single wall tube; and multiwall nanotubes (MWCNTs), which consist in several concentric walls, one inside the other.

A key factor for the reinforcement efficiency in a composite it is the interface bonding between the CNTs and the matrix. This work presents a new constitutive model to predict the mechanical performance of composites made of a thermo-plastic matrix reinforced with CNTs. The model takes into account explicitly the mechanical contribution of the interface between the matrix and the CNTs (F. Otero et. al., *Comp Structures*, 94:2920-2930 (2012)). The constitutive model is based in the mixing theory, which obtains the composite performance from the response of each constituent component, each one simulated with its own constitutive law. The model has been implemented into an in-house FEM code: PLCd.

As an application example, this code is used to predict the mechanical properties of a straight beam with different material configurations. In this case, a viscoelastic constitutive model is proposed for the polymeric matrix. The viscous response within the elastic range of the materials is studied. This response shows a high capacity of energy dissipation in composites reinforced with MWCNTs.

1 INTRODUCTION

Nanotubes obtained by arc-discharge (Cadek et al., 2002b) have Young modulus values in the order of 1TPa. Recent measurements carried out in arc-MWCNTs (multiwall nanotubes made by arc-discharge) have provide Young modulus values with values varying from 0.27 to 0.95 TPa, ultimate strain values higher than 12%, and ultimate tensile stresses in the range of 11 to 63 GPa (Yu et al., 2000). In these measurements it was also obtained the stress-strain curve of the MWCNT with help an electric microscope.

The properties obtained for CVD-MWCNT (multiwall carbon nanotubes obtained by Chemical Vapor Deposition) are low due to the defects in the nanotubes surface. The firsts Young modulus measurement known was made with an atomic force microscope (AFM) (Salvetat et al., 1999) and the values obtained were in the range of 12 to 50 GPa. Later on, new measurements have shown Young modulus values in order of 0.45 TPA, and ultimate tensile stresses of 3.6 GPa (Xie et al., 2000). The lower measured values were associated with defects in the nanotube and with the slipping of the inner tubes in MWCNTs. The difference in measured values between CVD-MWCNT and arc-MWCNT shows the influence of defects on the properties of these new materials.

It is not entirely clear which nanotube type performs better as a reinforcement. A recent study made by Cadek et al. (2004) comparing the properties of a polyvinylalcohol (PVA) matrix reinforced with different types of CNTs nanotubes (double wall nanotubes (DWCNT), SWCNT, arc-MWCNT and CVD-MWCNT) showed that the effectiveness of reinforcement is inversely proportional to its diameter, except when using SWCNT. The study also proved that the composite properties are proportional to the total interface area. The composite reinforced with SWCNT had the lowest properties; this result is associated with slipping of SWCNT inside the bundles. Finally, the study states that the best properties are obtained with the CVD-MWCNT with smaller diameter.

When there are not covalent bonds, the interaction between matrix and nanotube is made with Van der Waals forces. Several studies show that this union is weaker. Molecular Dynamics simulations made by Frankland et al. (2002) predicted values of the interfacial shear strength (IFSS) that do not exceed 2.8 MPa. Another study made by Liao and Li (2001) predicted values up to 160 MPa. According to Lordi and Yao (2000), the differences in the results depend on the polymer type and they can be in the range of 80 to 135 Mpa. The difference in the results, and the good values of IFSS, were attributed to the morphology and the capacity of the matrix to generate helical chains around the nanotube. On the other hand, nanotubes have a smoother outer surface and therefore, the contribution of the frictional forces to the IFSS are an order of magnitude lower (Barber et al., 2004).

Experimental results of pull-out tests show values of IFSS between 20-90 MPa (Barber et al., 2003, 2004). Other experiments using the drag-out technique have shown values between 35-376 MPa (Cooper et al., 2002). The disparity of the results suggests that is not always possible to generate covalent bonds. The maximum values obtained experimentally are associated to covalent bonds and consider that the interface zone has better properties than the rest of the matrix.

The above description shows that the final properties of the composite depend on many parameters. Together with these, there are others aspects that may also condition the final properties of the composite, such as the ondulation and misalignment of the nanotubes inside the matrix. All this variability can be considered the responsible of not having yet an accepted theory capable of describing correctly the performance of nanotube-reinforced composites. It

is also the reason because the existing theories fail in their predictions. Comparisons between measured mechanical properties and theoretical results, show that the theoretical predictions are generally three times higher than measured results (Sandler et al., 2002; Deng et al., 2007).

The constitutive model presented is based in the classical mixing theory. This theory obtains the mechanical performance of the composite from the behaviour of the composite constituents, each one simulated with its own constitutive law (Car et al., 2000). As it is written, the theory can be understood as a constitutive equation manager. The constitutive model is formulated with the same philosophy, which increases its versatility and simulation capability. The formulation is capable of predicting the response of the composite fairly accurately, requiring only the calibration of the mechanical properties of the interface.

2 DESCRIPTION OF CONSTITUTIVE MODEL

The model assumes that the composite is the combination of three different materials: matrix, CNTs and an interface (Coleman et al., 2006). The interface corresponds to the matrix that surrounds the CNTs. It is considered as an independent component, with its own constitutive law. The interface is used to define the capacity of the matrix to transfer the loads to the reinforcement.

Although the phenomenological performance of the composite already justifies the definition of an interface material; images obtained with Scanning Electron Microscope (SEM) of CNTs reinforced composites, such the ones shown in Figure 1, prove its actual existence. These images reveal that the structures protruding from the fractured surface have larger diameters than the original MWCNTs used in the sample preparation (Ding et al., 2003). The material surrounding the CNTs corresponds to the interface. The presence of an interface, as a differentiable material, is also proved by Differential Scanning Calorimetry (DSC) measurements carried out in composites with a semi-crystalline polymer as matrix. These measurements show a linear increase of crystalline matrix as the nanotube volume fraction increases, suggesting that each nanotube has a crystalline coating (Cadek et al., 2002a).

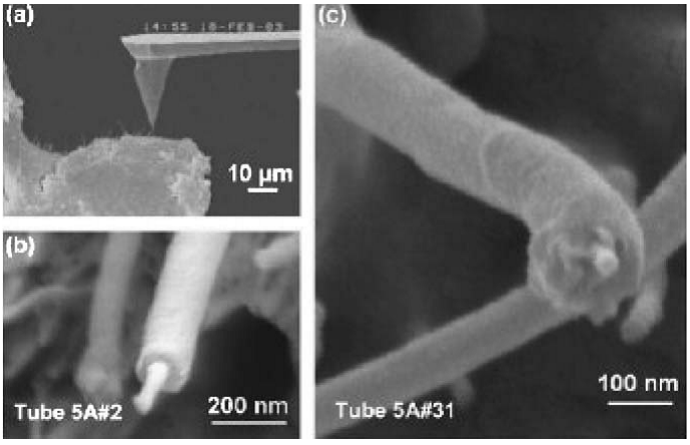

Figure 1: SEM image of nanomanipulation and fracture surface of composites (Ding et al., 2003).

Finally, the procedure proposed is summarized in Figure 2. This figure shows that the composite is divided in several layers, each one containing carbon nanotubes with a different orientation. All layers are coupled together using the parallel mixing theory. This is, assuming that all layers have the same deformation. The formulation developed provides the mechanical performance of each layer by combining the response of the three coexisting materials: ma-

trix, interface and CNTs. The layer response depends on the materials and on their volumetric participation in the composite.

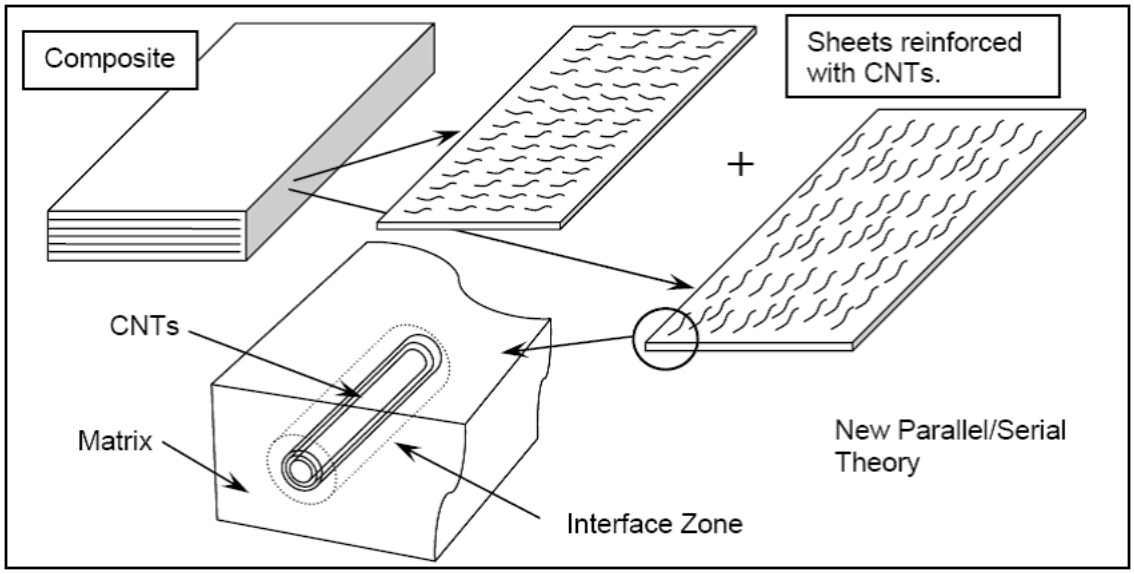

Figure 2: Representation of formation for reinforced composite.

First, the composite is split into matrix and a new material that results of coupling the CNTs with the interface. The relation between the matrix and the CNT-interface material is established in terms of the parallel mixing theory (they are assumed to have an iso-strain behaviour). On the other hand, CNTs and the interface are coupled together with a combination of parallel and serial mixing theories. The serial mixing theory assumes that all components have the same stresses.

Figure 3 shows scheme used to obtain the performance of the CNT-interface material. This is based in the short-fiber model developed by Jayatilaka (1979). According to this model, the load is transferred from the interface to the nanotube at the ends of the reinforcement, through shear stresses. In this region normal stresses in the fiber increase from zero to their maximum value, which is reached in the central part of the reinforcement. In this region there is not load transfer and shear stresses are null. This whole stress transfer scheme can be simplified assuming a CNT-interface performance defined by a serial mixing theory at the ends of the reinforcement and a parallel mixing theory at the center of it.

A parallel factor named N^{par} is defined to differentiate these two regions. This parameter, multiplied by the nanotube length, provides the length of the nanotube-interface element with a parallel behaviour. The length with a serial performance is defined by the complementary factor.

3 FORMULATION OF THE CONSTITUTIVE MODEL

The Helmholtz free energy (Malvern, 1969) of a material point subjected to small deformations can be described with the following thermodynamic formulation (Oller et al., 1996; Lubliner et al., 1989),

$$\Psi = \Psi\left(\varepsilon, \theta, \alpha\right) \tag{1}$$

where ε is the deformation tensor, θ a measure of temperature and $\alpha = \{\varepsilon^p, d, s\}$ a set of inner

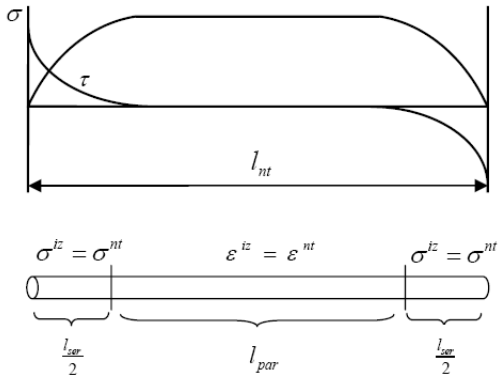

Figure 3: Different regions in the new material CNT-interface.

variables, for example: ε^p is the plastic deformation, d damage inner variable and s any other material internal variables.

The model proposed to simulate the composite combines the different components using the serial and parallel mixing theories. If this combination is performed according to what has been described in previous section, the expression of the Helmholtz free energy may be written as:

$$\Psi = k_m \Psi_m + (k_{nt} + k_{iz}) \left[\underbrace{N^{par} \left(\overline{k}_{nt} \Psi_{nt} + \overline{k}_{iz} \Psi_{iz} \right)}_{\tilde{\Psi}^{par}_{ntiz}} + \underbrace{(1 - N^{par}) \left(\overline{k}_{nt} \Psi_{nt} + \overline{k}_{iz} \Psi_{iz} \right)}_{\tilde{\Psi}^{ser}_{ntiz}} \right] \tag{2}$$

where Ψ_m, Ψ_{nt} and Ψ_{iz} are the specific Helmoholtz free energy for the matrix, the nanotube and the interface components, respectively; k_m, k_{nt} and k_{iz} are the volume fraction of each component, N^{par} is the parallel factor and,

$$\overline{k}_{nt} = \frac{k_{nt}}{k_{nt} + k_{iz}} \qquad \overline{k}_{iz} = \frac{k_{iz}}{k_{nt} + k_{iz}} \tag{3}$$

are the volume fractions of the carbon nanotubes and the interface in the new CNT-interface material. These volume fractions must verify:

$$k_m + k_{nt} + k_{iz} = 1 \qquad \overline{k}_{nt} + \overline{k}_{iz} = 1 \tag{4}$$

The relation among the strain tensors of the different components is:

$$\varepsilon = \varepsilon_m = \varepsilon^{par}_{ntiz} = \varepsilon^{ser}_{ntiz} \tag{5}$$

being ε and ε_m the composite and matrix deformations, respectively; ε^{par}_{ntiz} the deformation the new CNT-interface material with a parallel behavior; and ε^{ser}_{ntiz} the deformation of the CNT-interface material with a serial behavior.

The tangent constitutive tensor of the composite material may be derived from Eq. (2),

$$C = \frac{\partial^2 \Psi}{\partial \varepsilon \otimes \partial \varepsilon} = k_m \frac{\partial^2 \Psi_m}{\partial \varepsilon_m \otimes \partial \varepsilon_m} + \frac{\partial^2 \tilde{\Psi}^{par}_{ntiz}}{\partial \varepsilon^{par}_{ntiz} \otimes \partial \varepsilon^{par}_{ntiz}} + \frac{\partial^2 \tilde{\Psi}^{ser}_{ntiz}}{\partial \varepsilon^{ser}_{ntiz} \otimes \partial \varepsilon^{ser}_{ntiz}} \tag{6}$$

A parallel behavior means that all composite constituents have the same strain value. Therefore:

$$\varepsilon^{par}_{ntiz} = \varepsilon_{nt} = \varepsilon_{iz} \quad \Rightarrow \quad \frac{\partial^2 \tilde{\Psi}^{par}_{ntiz}}{\partial \varepsilon^{par}_{ntiz} \otimes \partial \varepsilon^{par}_{ntiz}} = N^{par} \left[\overline{k}_{nt} C_{nt} + \overline{k}_{iz} C_{iz} \right] = N^{par} C^{par}_{ntiz} \tag{7}$$

And a serial behavior means that all composite constituents have the same stress value. Thus:

$$\sigma^{ser}_{ntiz} = \sigma_{nt} = \sigma_{iz} \quad \Rightarrow \quad \varepsilon_{nt} = C^{-1}_{nt} : C^{ser}_{ntiz} : \varepsilon^{ser}_{ntiz} \quad ; \quad \varepsilon_{iz} = C^{-1}_{iz} : C^{ser}_{ntiz} : \varepsilon^{ser}_{ntiz} \tag{8}$$

$$\frac{\partial^2 \tilde{\Psi}^{ser}_{ntiz}}{\partial \varepsilon^{ser}_{ntiz} \otimes \partial \varepsilon^{ser}_{ntiz}} = (1 - N^{par}) \left[\overline{k}_{nt} C^{-1}_{nt} + \overline{k}_{iz} C^{-1}_{iz} \right]^{-1} = (1 - N^{par}) C^{ser}_{ntiz} \tag{9}$$

Replacing Eq. (7) and Eq. (9) in Eq. (6) it is possible to obtain a simplified expression of the tangent constitutive tensor:

$$C = k_m C_m + (k_{nt} + k_{iz}) \left[N^{par} C^{par}_{ntiz} + (1 - N^{par}) C^{ser}_{ntiz} \right] \tag{10}$$

3.1 Definition of the parallel factor

The parallel factor is defined as,

$$N^{par} = \frac{l_{par}}{l_{nt}} \quad , \quad 0 \leq N^{par} \leq 1 \tag{11}$$

where l_{nt} is the length of the nanotube and l_{par} is function of geometry and mechanical properties of the nanotube and the interface. The value of this length can be obtained from the equation of tension distribution in a reinforcement considering perfect bond with the matrix, which is (Jayatilaka, 1979):

$$\sigma_{nt}(x) = E_{nt} \left[1 - \frac{\cosh\left(\beta \left(l_{nt} - 2x \right)\right)}{\cosh\left(\beta l_{nt}\right)} \right] \varepsilon_m \qquad \beta = \sqrt{\frac{2G_{iz}}{E_{nt} d^2_{nt} \ln\left(1 + \frac{b}{r_{nt}}\right)}} \tag{12}$$

where x represents the longitudinal positions in the reinforcement, and the subscripts "nt" and "iz" refers to the properties of nanotube and interface zone, respectively. E and G are the Young's modulus and the shear Modulus, and b is the thickness material arround of the CNTs associated wiht the interface zone.

Defining $l_{par} = l_{nt} - 2x$, its value can be obtained by finding the position "x" for which the effective modulus obtained from the integration of the tension distribution becomes:

$$E_{eff} = \frac{l_{par}}{l_{nt}} E^{par}_{ntiz} + \left(1 - \frac{l_{par}}{l_{nt}} \right) E^{ser}_{ntiz} \tag{13}$$

This procedure provides a value of the parallel length of:

$$l_{par} = \frac{1}{\beta} \cosh^{-1} \left[\frac{1}{3} \cosh\left(\beta l_{nt}\right) \right] \tag{14}$$

3.2 Constitutive model for a single material

The formulation developed require all composite components to fulfill equation 1. Therefore, it is possible to use any constitutive law to describe the mechanical performance of the different components. However, for the sake of simplicity, in the following are defined the three specific models that will be used for each composite component.

3.2.1 Constitutive model for matrix material

Matrix material is defined with an elastoplastic law. The specific Helmholtz free energy for this material, considering uncoupled elasticity is:

$$\Psi\left(\varepsilon^e, p, \theta\right) = \Psi^e\left(\varepsilon^e\right) + \Psi^p\left(p\right) + \Psi^t\left(\theta\right) = \frac{1}{2}\varepsilon^e : C : \varepsilon^e + \Psi^p\left(p\right) + \Psi^t\left(\theta\right) \tag{15}$$

where Ψ^e is the specific elastic free energy, Ψ^p is the specific plastic free energy, Ψ^t is the specific temperature free energy, p is a internal variable tensor associated with plastic behaviour. The total deformation of the material tensor is split into its elastic, ε^e and plastic, ε^p parts. This is:

$$\varepsilon = \varepsilon^e + \varepsilon^p \tag{16}$$

The local form of the Clausius-Duhem inequality for this material can be expressed as:

$$\Xi = \sigma : \dot{\varepsilon} - \eta\dot{\theta} - \dot{\Psi} - \frac{1}{\theta} q . \frac{\partial \theta}{\partial x} \geq 0 \tag{17}$$

$$\sigma : \left(\dot{\varepsilon}^e + \dot{\varepsilon}^p\right) - \eta\dot{\theta} - \left[\frac{\partial \Psi^e}{\partial \varepsilon^e} : \dot{\varepsilon}^e + \frac{\partial \Psi^p}{\partial p} . \dot{p} + \frac{\partial \Psi^t}{\partial \theta}\dot{\theta}\right] - \frac{1}{\theta} q . \frac{\partial \theta}{\partial x} \geq 0 \tag{18}$$

$$\left(\sigma - \frac{\partial \Psi^e}{\partial \varepsilon^e}\right) : \dot{\varepsilon}^e - \left(\eta + \frac{\partial \Psi^t}{\partial \theta}\right)\dot{\theta} + \sigma : \dot{\varepsilon}^p - \frac{\partial \Psi^p}{\partial p} . \dot{p} - \frac{1}{\theta} q . \frac{\partial \theta}{\partial x} \geq 0 \tag{19}$$

being σ the stress tensor, η the entropy, and q the vector field of heat flow. To ensure compliance with the second thermodynamic law it must be defined,

$$\sigma \doteq \frac{\partial \Psi^e}{\partial \varepsilon^e} \qquad \eta \doteq -\frac{\partial \Psi^t}{\partial \theta} \qquad P \doteq -\frac{\partial \Psi^p}{\partial p} \tag{20}$$

where P is the thermodynamic tensor associated with the internal variable tensor p. Finally, the mechanical dissipation for a material point is,

$$\Xi_m = \Xi_p = \sigma : \dot{\varepsilon}^p + P . \dot{p} \geq 0 \tag{21}$$

3.2.2 Constitutive model for interface material

The interface region is simulated with a damage material. In this case, the expression of the Helmholtz free energy is,

$$\Psi\left(\varepsilon, d, \theta\right) = \Psi^e\left(\varepsilon, d\right) + \Psi^t\left(\theta\right) = \left(1 - d\right)\Psi_o^e\left(\varepsilon\right) + \Psi^t\left(\theta\right) = \left(1 - d\right)\frac{1}{2}\varepsilon : C : \varepsilon + \Psi^t\left(\theta\right) \tag{22}$$

where d is a internal variable associated with the damage. The local form of the Clausius-Duhem inequality Eq.17 for this material can be expressed as,

$$\sigma : \dot{\varepsilon} - \eta\dot{\theta} - \left[\frac{\partial \Psi^e}{\partial \varepsilon} : \dot{\varepsilon} + \frac{\partial \Psi^e}{\partial d}\dot{d} + \frac{\partial \Psi^t}{\partial \theta}\dot{\theta}\right] - \frac{1}{\theta} q . \frac{\partial \theta}{\partial x} \geq 0 \tag{23}$$

$$\left(\sigma - \frac{\partial \Psi^e}{\partial \varepsilon}\right) : \dot{\varepsilon} - \left(\eta + \frac{\partial \Psi^t}{\partial \theta}\right)\dot{\theta} - \frac{\partial \Psi^e}{\partial d}\dot{d} - \frac{1}{\theta} q . \frac{\partial \theta}{\partial x} \geq 0 \tag{24}$$

To ensure compliance with the second thermodynamic law it must be defined:

$$\sigma \doteq \frac{\partial \Psi^e}{\partial \varepsilon} \qquad \eta \doteq -\frac{\partial \Psi^t}{\partial \theta} \qquad D \doteq -\frac{\partial \Psi^e}{\partial d} \tag{25}$$

being D the thermodynamic scalar associated with the internal scalar variable d. And, the mechanical dissipation for a material point is:

$$\Xi_m = \Xi_d = D.\dot{d} \geq 0 \tag{26}$$

3.2.3 Constitutive model for nanotubes

Nanotubes are considered elastic. In this case the Helmholtz free energy can be written as,

$$\Psi(\varepsilon, \theta) = \Psi^e(\varepsilon) + \Psi^t(\theta) = \frac{1}{2}\varepsilon : C : \varepsilon + \Psi^t(\theta) \tag{27}$$

And the local form of the Clausius-Duhem inequality Eq.17 can be expressed in this case as,

$$\sigma : \dot{\varepsilon} - \eta\dot{\theta} - \left[\frac{\partial \Psi^e}{\partial \varepsilon} : \dot{\varepsilon} + \frac{\partial \Psi^t}{\partial \theta}\dot{\theta}\right] - \frac{1}{\theta} q . \frac{\partial \theta}{\partial x} \geq 0 \tag{28}$$

$$\left(\sigma - \frac{\partial \Psi^e}{\partial \varepsilon}\right) : \dot{\varepsilon} - \left(\eta + \frac{\partial \Psi^t}{\partial \theta}\right)\dot{\theta} - \frac{1}{\theta} q . \frac{\partial \theta}{\partial x} \geq 0 \tag{29}$$

To ensure compliance with the second thermodynamic law,

$$\sigma \doteq \frac{\partial \Psi^e}{\partial \varepsilon} \qquad \eta \doteq -\frac{\partial \Psi^t}{\partial \theta} \tag{30}$$

Equivalent properties for MWCNTs

MWCNTs consist of concentric SWCNTs joined together with relatively weak van der Waals forces. For this reason, the capacity to transfer the load from the external wall to the internal walls is low. Some papers Thostenson and Chou (2003); Zhou et al. (2004) propose to simulate the CNTs like a solid cylinder with same exterior diameter and length, but with effective properties. The effective properties are obtained assuming that the outer wall takes the total load. In this approach it is assumed that the properties of the outer wall correspond to those of a graphite sheet. The effective stiffness of the MWCNTs is calculated by imposing that for a same applied force, the deformation must be the same:

$$\bar{\varepsilon}_{nt} = \varepsilon_{nt} \quad \Rightarrow \quad \bar{E}_{nt} = \frac{A_{ow}}{\bar{A}_{nt}} E_g \tag{31}$$

where $\bar{E}_{nt}$ and E_g are the Young's modulus of the effective solid nanotube and graphite sheet, respectively, and $\bar{A}_{nt}$ and A_{ow} are the areas of the effective solid nanotube and outer wall, respectively. Equation 31 can be also read as,

$$\bar{E}_{nt} = \left[1 - \left(1 - \frac{2t}{d_{nt}}\right)^2\right] E_g \qquad , \qquad \frac{t}{d_{nt}} \leq 0.5 \tag{32}$$

being t the thickness of one wall in the MWCNTs and d_{nt} is the external diameter of the MWCNTs.

Using the same procedure it is possible to obtain the shear modulus of the solid cylinder, by forcing the same twist when applying the same torque (T).

$$\bar{\phi}_{nt} = \phi_{nt} \quad \Rightarrow \quad \frac{T l_{nt}}{\bar{G}_{nt}\bar{J}_{nt}} = \frac{T l_{nt}}{G_g J_{ow}} \quad \Rightarrow \quad \bar{G}_{nt} = \frac{J_{ow}}{\bar{J}_{nt}} G_g \tag{33}$$

where $\bar{G}_{nt}$ and G_g are the shear modulus of the effective solid CNTs and graphite sheet, respectively, and $\bar{J}_{nt}$ and J_{ow} are the polar moment of inertia of the effective solid CNTs and outer wall, respectively.

$$\bar{J}_{nt} = \frac{\pi d_{nt}^4}{32} \quad , \quad J_{ow} = \frac{\pi\left(d_{nt}^4 - (d_{nt} - 2t)^4\right)}{32} \tag{34}$$

Replacing the expressions of Eq. 34 in Eq. 33, the equivalent shear modulus can be written as,

$$\bar{G}_{nt} = \left[1 - \left(1 - \frac{2t}{d_{nt}}\right)^4\right] G_g \tag{35}$$

Finally, it is necessary to obtain the new density of the effective solid CNTs, as the total weight of the MWCNTs can not change in the composite when they are considered a solid cylinder.

$$\bar{\rho}_{nt} = \frac{A_{nt}}{\bar{A}_{nt}} \rho_g \quad \Rightarrow \quad \bar{\rho}_{nt} = \left[1 - \left(\frac{d_i}{d_{nt}}\right)^2\right] \rho_g \tag{36}$$

being ρ_g the density of the graphite sheet ($\rho_g = 2.25\ [g\,cm^{-3}]$) and d_i the internal diameter of the MWCNTs.

The most common parameter used to define the amount of CNTs added to a composite is their weight fraction. However, the numerical model developed requires knowing the volume fraction. The volumen fraction of CNTs in the composite is the volume that occupies a solid cilinder with the same external diameter. This parameter can be calculated with the following expresion (Thostenson and Chou, 2003).

$$k_{nt} = \frac{w_{nt}}{w_{nt} + \frac{\bar{\rho_{nt}}}{\rho_m} - \frac{\bar{\rho_{nt}}}{\rho_m} w_{nt}} \tag{37}$$

where w_{nt} is the weight fraction and ρ_m is the density of the matrix.

4 MATERIAL NON-LINEARITY OF THE PROPOSED MODEL

If a constituent (i.e. the interface) is simulated with a non-linear law, the whole composite will become non-linear. As it has been already explained, with the present model it is possible to use any non-linear formulation to simulate the constituents, such as plasticity, damage, viscosity, etc.

Besides the non-linear performance provided by each constituent, the load transfer capacity of the interface region is also affected if the interface is damaged. This effect must be included in the formulation.

According to Figure 3, the load is transferred from the interface to the CNTs reinforcements at their ends. Interface damage is expected to occur at the ends of the reinforcement, where there is larger stress concentrations. Assuming that the damaged region is unable to transfer loads and that the length required to transfer loads must remain constant, interface damage ends up affecting the parallel length of the nanotube, which can be calculated as:

$$l_{par} = l^o_{par}\,(1 - d) \tag{38}$$

where l^o_{par} is the initial length of the nanotube working in parallel and d is the interface damage.

The dependence of the parallel length on the interface material damage provides a non-linear response of the composite, even when matrix and the carbon nantotube reinforcement are in their linear range.

5 NUMERICAL IMPLEMENTATION

The proposed model has been implemented in PLCd , a finite element code that works with 3D solid geometries (PLCd-Manual, 1991-to present). PLCd has already implemented the constitutive laws that will be used to predict the performance of the composite components (elasto-plastic, elasto-damage and elastic). The formulation has been written so that the constitutive laws of the constituents are seen as "black boxes", following the recommendations of Martinez et al. (2008) and Rastellini et al. (2008).

6 VALIDATION

This section presents the simulation of a four points bending beam made of three different PEEK materials. Two of them with different proportions of CNTs reinforcements and the third one without any reinforcement. This example is used to describe the numerical performance of the formulation proposed in this work.

6.1 Material Propierties

The material used in current simulation is a PEEK matrix reinforced with multiwall carbon nanotubes. In the following are described the properties of each constituent material.

6.1.1 Properties of Nanotubes

The MWCNTs (NC 7000) are provided by Nanocyl S.A. The geometric features are obtained from paper of Jiang et al. (2012), who defines as average diameter and length of 10.4 nm and 0.7 μm, respectively. The nanotube is considered an orthotropic material so its mechanical properties are different along the directions of each of the axes. These equivalent properties can

be estimated according to subsection 3.2.3, assuming $E_g = 1.05 \pm 0.05$ [TPa] and $t = 0.34$ nm and $G_g = 0.4 \pm 0.05$ [TPa] (Li and Chou, 2003):

$$E_1 = \bar{E}_{nt} = 131 \text{ GPa} \qquad G_{12} = G_{13} = \bar{G}_{nt} = 104 \text{ GPa}$$

$$v_{12} = v_{13} = v_{23} = v_{nt} = 0.2$$

The transversal properties of the nanotubes are assumed to be equal to the properties of the interface zone:

$$E_2 = E_3 = E_{iz} \qquad G_{23} = G_{iz}$$

$$v_{21} = \frac{E_2}{E_1} v_{12} \qquad v_{31} = \frac{E_2}{E_1} v_{13} \qquad v_{32} = \frac{E_3}{E_2} v_{23}$$

6.1.2 Properties of PEEK Matrix

For PEEK matrix we are using the following values. These have been taken from the M_RECT Project and from the information provided by the manufacturer (http://www.victrex.com):

$$E_m = 3.9 \text{ GPa} \qquad G_m = 1.9 \text{ GPa} \qquad v_m = 0.4$$

6.1.3 Properties of Interface Zone

The interface zone is associated with the crystalline matrix around of MWCNTs. The properties of this material are better than those of the amorphous matrix. The volume fraction of the interface zone has been estimated with data of M_RECT Project. The mechanical properties of the interface are obtained with the same procedure described in Coleman et al. (2006) and Otero et al. (2012) but using the data of Díez-Pascual et al. (2010a,b):

$$E_{iz} = 5.05 \text{ GPa} \qquad G_{iz} = 2.46 \text{ GPa} \qquad v_{iz} = 0.4$$

6.2 Composites Data

The composites have been made with the PEEK matrix reinforced with different weight fractions $(0.0, 0.5, 2.0\%)$ of MWCNTs . Table 1 shows the volumetric participations of each material in the composites simulated.

Composite	$K_m\%$	$K_{nt}\%$	$K_{iz}\%$
PEEK	100	-	-
PEEK-0.5%CNT	84.95	0.35	14.7
PEEK-2.0%CNT	91.89	1.41	6.70

Table 1: Composites data.

The MWCNTs orientation has been defined assuming that the composite is formed with different layers, each one with a specific angle and volume fraction. The particular MWCNTs distribution is the one presented in the Figure 4. The volume fractions shown in the figure are relative to the MWCNTs volume fraction used in the composite.

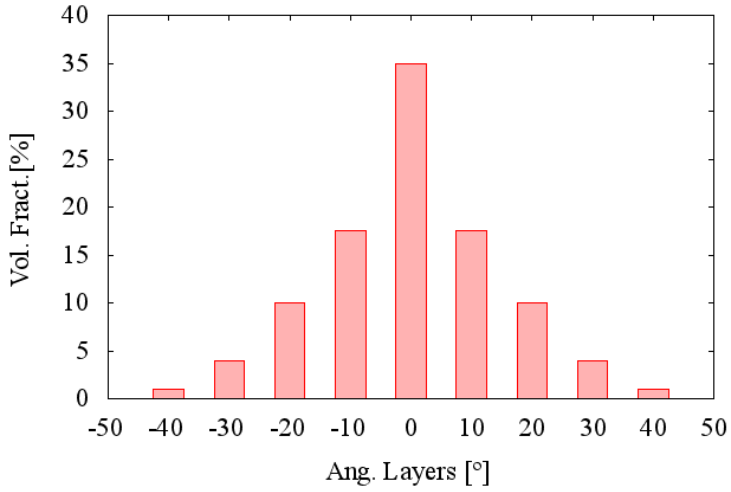

Figure 4: Nanotubes distribution in the composite.

6.3 Geometry of the analysed structure and FEM model

The structure selected for the numerical simulations is a simple supported beam. Two concentrated loads are applied at $1/3$ of both ends.

6.3.1 Geometry of the structurel

Figure 5 shows the geometry and the scheme of boundary conditions and applied loads of the analysed beam.

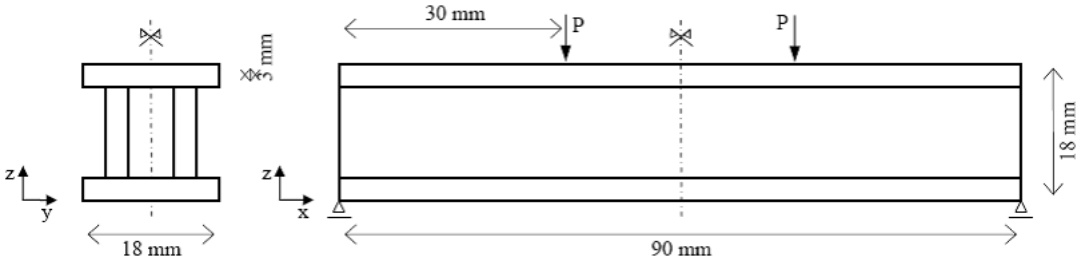

Figure 5: Geometry, boundary conditions and loading.

6.3.2 FEM model

The symmetry of the geometry, loading and boundary conditions of the beam to analyse allows a reduced FEM model ($1/4$ of the real geometry). In Table 2, it is shown the most relevant information concerning the mesh of the FEM model.

In order to obtain the real behaviour of the structure with the reduced FEM model it is necessary to impose the restrictions for symmetry. There are two symmetry planes: The symmetry plane that has X-axis as its normal (longitudinal axis) restricts displacement to zero in X direction over their nodes. The other symmetry plane has the Y-axis as its normal and imposes null displacements in Y direction over their nodes.

Item	Nodes	Elements	Type Elem.	Order
Quantity/Type	1953	1200	Hexahedron	Quadratic

Table 2: Mesh information.

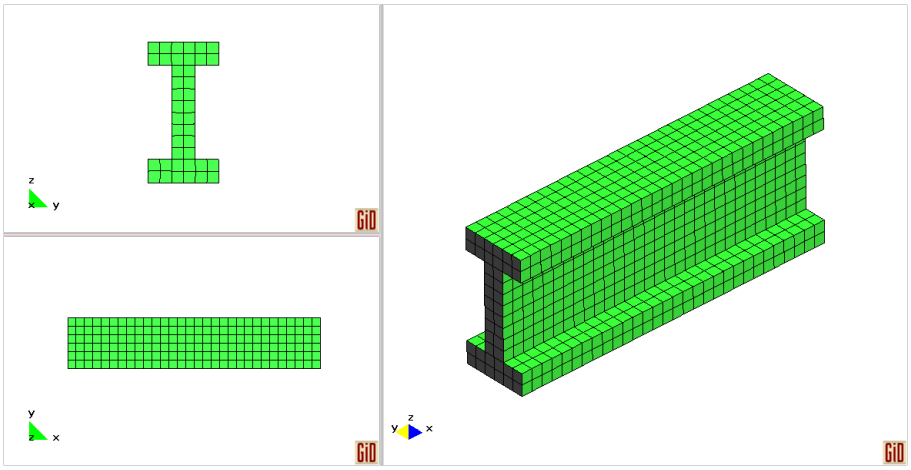

Figure 6: FEM model.

The orientation angles in the definition of the composite are referred to the X-axis.

6.4 Elastic Results

The numerical results obtained in the analysis are presented here in comparative form, taken the result obtained for the non-reinforced matrix as reference.

In all cases, the applied load for elastic analysis is a fixed displacement: -0.001 mm in Z direction at P position (see the figure of geometry). The result considered for comparison is the force reaction in Z direction in the support location. As the imposed displacement is the same for all analysis, the reaction force increases when the matrix is reinforced. Table 3 shows this variation in the maximum load applied, normalized by the maximum load in the non-reinforced matrix.

PEEK	PEEK-0.5%CNT	PEEK-2.0%CNT
1	1.20	1.52

Table 3: Limit elastic load obtained for each model, normalized by the limit load obtained for the non-reinforced PEEK model.

In the central section of the beam, between imposed loads, there is a pure bending situation. At both ends of the beam there are bending and shear loads. In Table 4, it is possible to see the longitudinal (X direction) and Shear (XZ direction) stresses for all models.

6.5 Non-linear analysis

In order to obtain the non-linear response of the structure it is necessary to simulate accurately the non-linear behaviour of the composite used in it. As it has been described in the theory

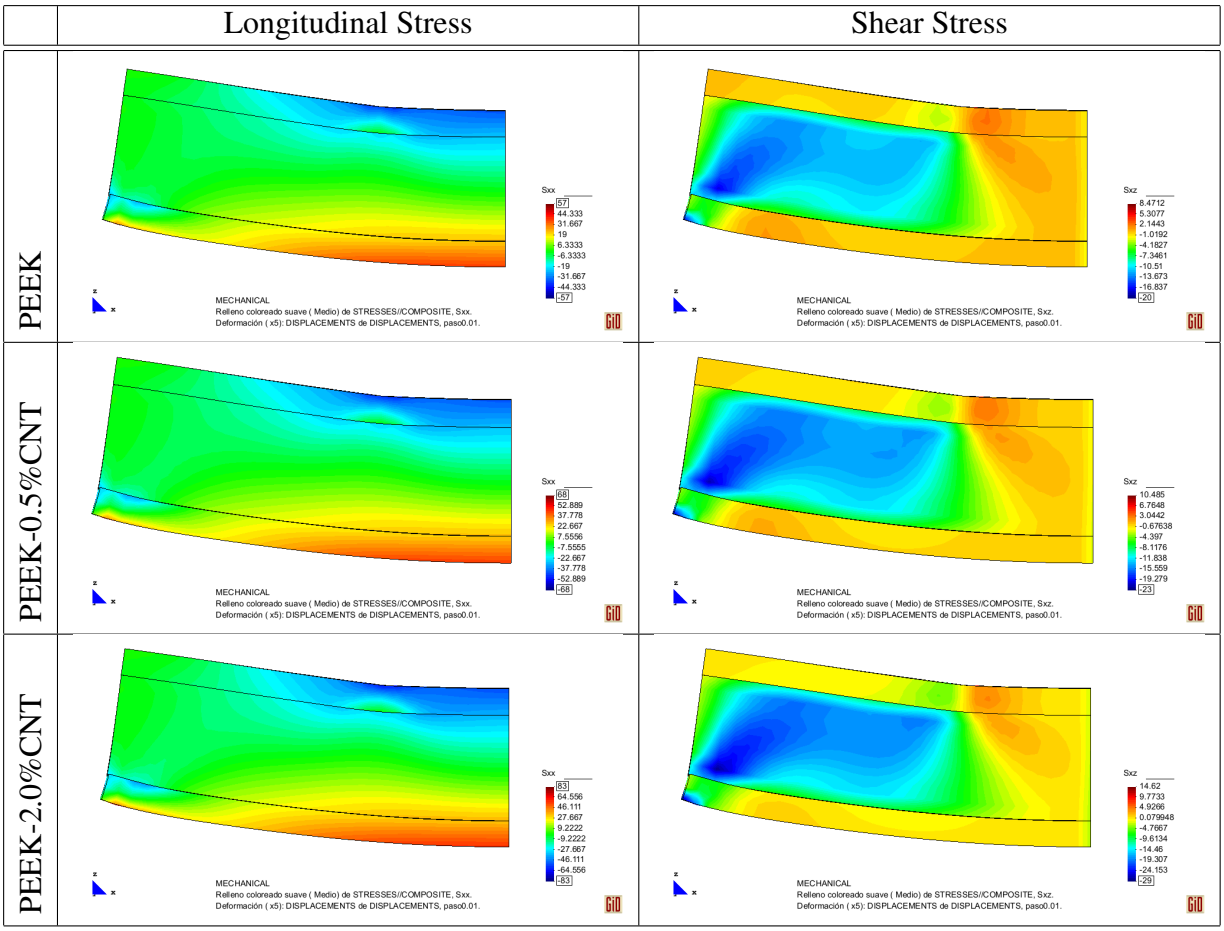

Table 4: Stress distribution for elastic results.

presented in previous section, the composite mechanical performance is determined by the behaviour of each constituent material. Each of these materials is characterized with a constitutive model that needs calibration.

6.5.1 PEEK Matrix

An elasto-plastic constitutive model with hardening is applied to typify the PEEK matrix. The model is calibrated with an initial yielding stress of 32 MPa and a ultimate strength of 90 MPa. With these values, Figure 7 compares experimental and numerical results.

6.5.2 Interface zone

An elasto-damage constitutive model with exponential softening is applied to characterize the PEEK interface zone. The model is calibrated to reproduce the experimental test of the composite (See Figure 8). The damge starts when the interface stress reachs to 28 MPa.

6.5.3 Nanotubes

The Nanotubes are considered to have a linear elastic behaviour.

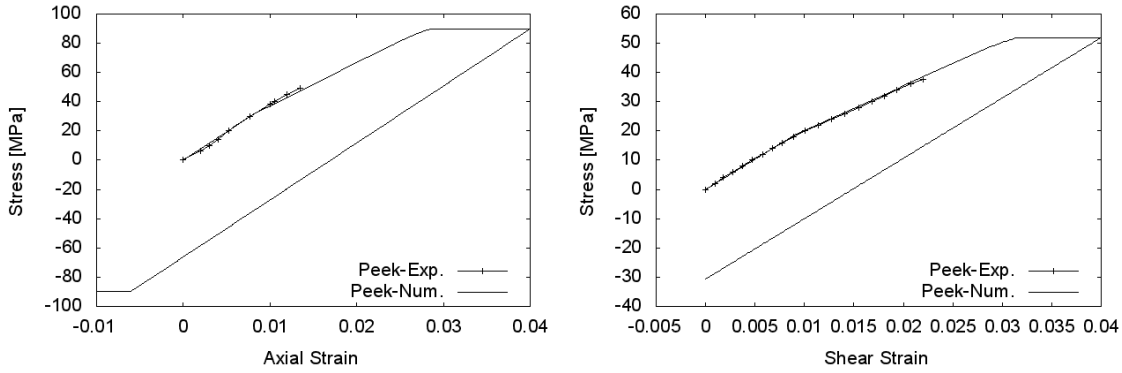

Figure 7: Behaviour of the PEEK constitutive model.

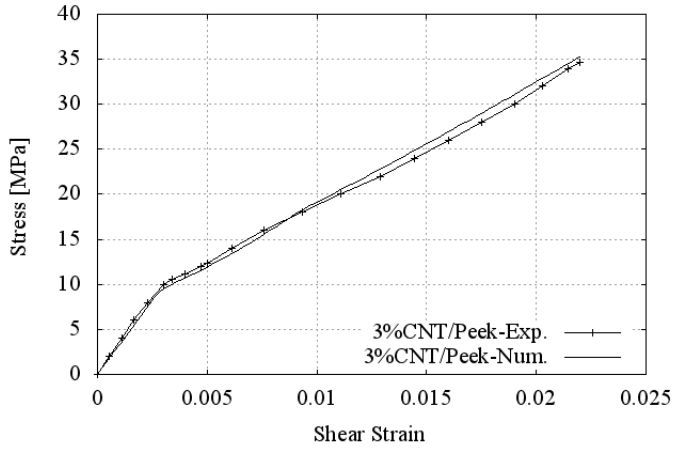

Figure 8: Behaviour of the interface zone constitutive model.

6.5.4 Global structural response

The structure is loaded as shown in Figure 5. The imposed displacement at position "P" is gradually increased while Z-reaction at the support assesses the vertical force that the structure is able to take. The total force is four times that Z-reaction due to FEM model symmetric considerations. The vertical (Z) displacement at the middle of the beam is measured as the loading increase.

The imposed displacement is applied in 100 load steps of 0.1 mm. Figure 9 shows the results obtained. When the vertical displacement is around 1.5 mm the curves show the first loss of stiffness, this is due to plasticity in the matrix at the middle of the beam. Then, when the vertical deformation is between 3 mm to 6 mm there is the second loss of stiffness, in this case, due to damage on the interface zone. Subsequently, it is possible to see that the structures with MWCNTs has less stiffness that the non-reinforced ones. This response is obtained because at this point interface zone is completely damaged and, therefore, the contribution of the MWCNTs to the global stiffness is null. The stiffness obtained is equivalent to the stiffness of plain PEEK matrix with some holes. This effect is observed clearly in Figure 10. This Figure shows the same curves that the Figure 9 extended up to a vertical displacement of 50 mm.

Figure 10 shows a new loss of stiffness that takes place from 30 mm to 40 mm of vertical displacement. This last loss of stiffness is due to matrix reaching its ultimate strength a the

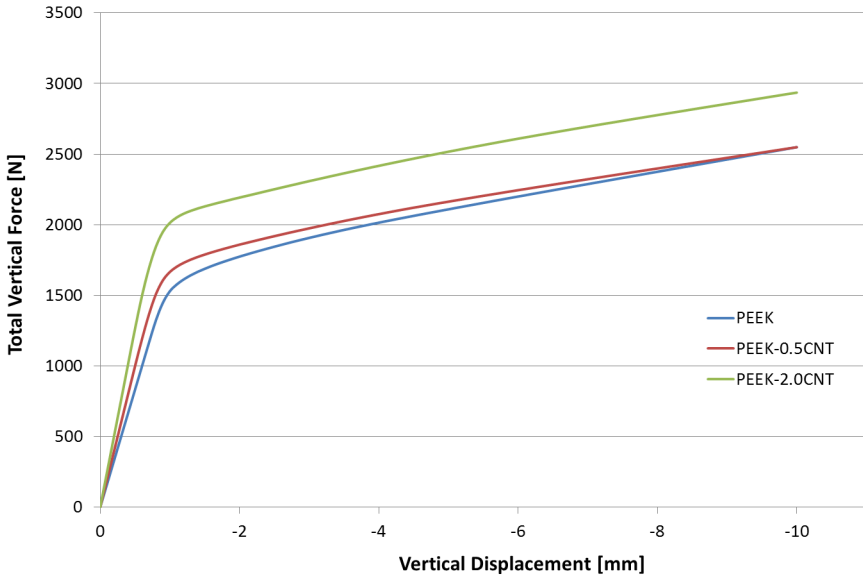

Figure 9: Structural response for PEEK-CNT.

middle of the beam.

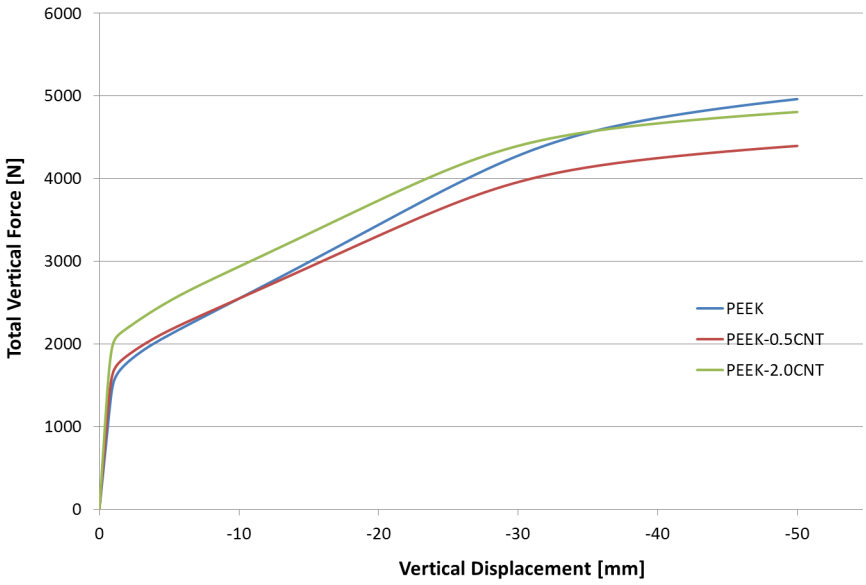

Figure 10: Structural response for PEEK-CNT up to 50 mm of vertical displacement.

Figure 11 shows the distribution of the longitudinal and the shear stresses for the composite reinforced with MWCNTs. The longitudinal plastic deformation and the equivalent stress for the composite are shown in Figure 12.

6.6 Visco-elastic analysis

In order to obtain a viscous response of the composite it is necessary to use a visco-elastic model to characterize its components. The visco-elastic model used for the matrix and the interface zone is the generalized Maxwell model. Figure 13 shows a scheme of the viscous

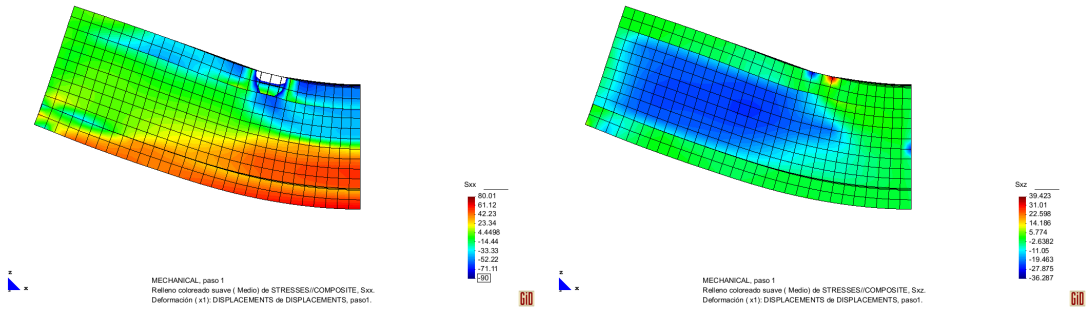

Figure 11: Longitudinal and shear stresses PEEK-CNT.

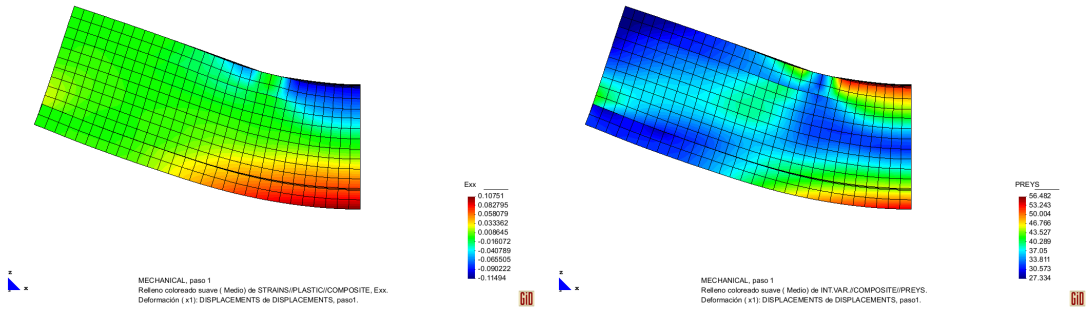

Figure 12: Longitudinal plastic deformation and equivalent stress in the composite.

model implemented in PLCd code. To conduct the visco-elastic analysis, the MWCNTs are considered to have a linear elastic behaviour.

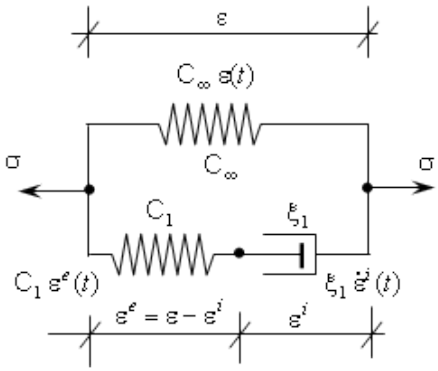

Figure 13: Generalized Maxwell model implemented.

The response obtained, after calibrating the model, is shown in Figure 14. This figure shows the stress-strain curve of a point inside of the structure in a complete load-unload cycle. The simulation has been conducted with the three different composites previously defined. This figure shows that the area enclosed in the load-unload cycle in the composites reinforced with carbon nanotubes is larger than if the matrix is not reinforced. In other words, the dissipation capacity of a composite with MWCNTs is better than when the matrix alone. The composite reinforced with 0.5% (weight fraction) of MWCNTs has higher dissipative capacity than the

other composite. This is because the volume fraction of the interface zone is higher than in the other composite, as it is shown in Table 1. This phenomenon occurs because when the volume fraction of the CNTs in the composite is low, their distribution in the composite improves, incresing the interface volume.

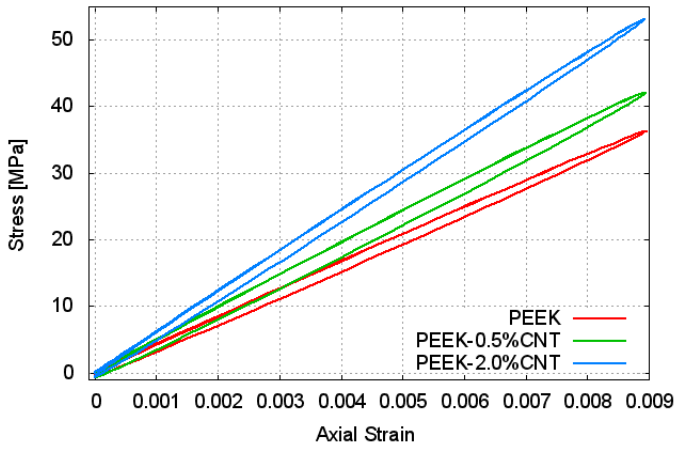

Figure 14: Structural response at 1 Hz.

7 CONCLUSIONS

The present work has presented a formulation based on the mixing theory, capable of predicting the mechanical performance of composites reinforced with carbon nanotubes. The model presented relates the CNTs and the matrix in which they are embedded, using an interface material. This approach makes possible to consider non-linear phenomenons, such as CNT debounding, by using non-linear constitutive laws to characterize the interface material. The formulation is written in a way in which all materials can be defined with their own constitutive law, improving the versatility of the model.

The formulation has used to predict and compare the mechanical properties of a straight beam subjected to four-point bending, with different material configurations. The non-linear analysis for the same structure has also been made. The non-linear response of the structure presents different points where there is a loss of stiffness, result of reaching the linear threshold of the different component materials.

A visco-elastic constitutive model is proposed for the polymeric matrix and the interface zone. The viscous response within the elastic range of the materials has been studied. The good capacity of energy dissipation in composites reinforced with MWCNTs has been proved with the simulations performed.

ACKNOWLEDGEMENTS

This work has been supported by the European Community under grant 246067, Multiscale Reinforcement of Semi-crystalline Thermoplastic Sheets and Honeycombs (M_RECT), NMP-2009-2.5-1 and “amb el suport de la Universitat Politècnica de Catalunya (UPC)”.

REFERENCES

Barber A.H., Cohen S.R., Kenig S., and Wagner H.D. Interfacial fracture energy measurements for multi-walled carbon nanotubes pulled from a polymer matrix. *Composites Science and Technology*, 64(15):2283–2289, 2004.

Barber A.H., Cohen S.R., and Wagner H.D. Measurement of carbon nanotube polymer interfacial strength. *Applied Physics Letters*, 82(23):4140–4142, 2003.

Cadek M., Coleman J.N., Barron V., Hedicke K., and Blau W.J. Morphological and mechanical properties of carbon nanotube reinforced semicrystalline and amorphous polymer composites. *Applied Physics Letters*, 81(27):5123–5125, 2002a.

Cadek M., Coleman J.N., Ryan K.P., Nicolosi V., Bister G., Fonseca A., Nagy J.B., Szostak K., Béguin F., and Blau W.J. Reinforcement of polymers with carbon nanotubes: the role of nanotube surface area. *Nano Letters*, 4(2):353–356, 2004.

Cadek M., Murphy R., McCarthy B., Drury A., Lahr B., Barklie R.C., in het Panhuis M., Coleman J.N., and Blau W.J. Optimisation of the arc-discharge production of multi-walled carbon nanotubes. *Carbon*, 40(6):923–928, 2002b.

Car E., Oller S., and Oñate E. An anisotropic elastoplastic constitutive model for large strain analysis of fiber reinforced composite materials. *Computer Methods in Applied Mechanics and Engineering*, 185(2-4):245–277, 2000.

Coleman J.N., Cadek M., Ryan K.P., Fonseca A., Nagy J.B., Blau W.J., and Ferreira M.S. Reinforcement of polymers with carbon nanotubes. the role of an ordered polymer interfacial region. experiment and modeling. *Polymer*, 47(26):8556–8561, 2006.

Cooper C.A., Cohen S.R., Barber A.H., and Wagner H.D. Detachment of nanotubes from a polymer matrix. *Applied Physics Letters*, 81(20):3873–3875, 2002.

Deng F., Ogasawara T., and Takeda N. Tensile properties at different temperature and observation of micro deformation of carbon nanotubes poly(ether ether ketone) composites. *Composites Science and Technology*, 67(14):2959–2964, 2007.

Díez-Pascual A., Naffakh M., González-Domínguez J., Ansón A., Martínez-Rubi Y., Martínez M., Simard B., and Gómez M. High performance peek/carbon nanotube composites compatibilized with polysulfones-i. structure and thermal properties. *Carbon*, 48:3485–3499, 2010a.

Díez-Pascual A., Naffakh M., González-Domínguez J., Ansón A., Martínez-Rubi Y., Martínez M., Simard B., and Gómez M. High performance peek/carbon nanotube composites compatibilized with polysulfones-ii. mechanical and electrical properties. *Carbon*, 48:3500–3511, 2010b.

Ding W., Eitan A., Fisher F.T., Chen X., Dikin D.A., Andrews R., Brinson L.C., Schadler L.S., and Ruoff R.S. Direct observation of polymer sheathing in carbon nanotube polycarbonate composites. *Nano Letters*, 3(11):1593–1597, 2003.

Frankland S.J.V., Caglar A., Brenner D.W., and Griebel M. Molecular simulation of the influence of chemical cross-links on the shear strength of carbon nanotube-polymer interfaces. *The Journal of Physical Chemistry B*, 106(12):3046–3048, 2002.

Jayatilaka A.S. *Fracture of engineering brittle materials*. Applied Sciences, London, 1979.

Jiang Z., Hornsby P., McCool R., and Murphy A. Mechanical and thermal properties of polyphenylene sulfide/multiwalled carbon nanotube composites. *Journal of applied polymer science*, 123:2676–2683, 2012.

Li C. and Chou T. Elastic moduli of multi-walled carbon nanotubes and the affect of van der waals forces. *Composites Science and Technology*, 63:1517–1524, 2003.

Liao K. and Li S. Interfacial characteristics of a carbon nanotube–polystyrene composite system. *Applied Physics Letters*, 79(25):4225–4227, 2001.

Lordi V. and Yao N. Molecular mechanics of binding in carbon-nanotube-polymer composites. *Journal of Materials Research*, 15(12):2770–2779, 2000.

Lubliner J., Oliver J., Oller S., and Oñate E. A plastic damage model for concrete. *International Journal of Solids and Structures*, 25(3):299–326, 1989.

Malvern L.E. *Introduction to the mechanics of a continuous medium*. 1969. ISBN 134876032.

Martinez X., Oller S., Rastellini F., and Barbat A.H. A numerical procedure simulating rc structures reinforced with frp using the serial/parallel mixing theory. *Computers and Structures*, 86:1604–1618, 2008.

Oller S., Oñate E., Miquel J., and Botello S. A plastic damage constitutive model for composite materials. *International Journal of Solids and Structures*, 33(17):2501–2518, 1996.

Otero F., Martínez X., Oller S., and Salomón O. Study and prediction of the mechanical performance of a nanotube-reinforced composite. *Composites Structures*, 94:2920–2930, 2012.

PLCd-Manual. *Non-linear thermomachanic finite element code oriented to PhD student education*. Code developed at CIMNE, 1991-to present.

Rastellini F., Oller S., Salomón O., and Oñate E. Composite materials non-linear modelling for long fibre-reinforced laminates continuum basis, computational aspect and validations. *Computers and Structures*, 86:879–896, 2008.

Salvetat J.P., Kulik A.J., Bonard J.M., Briggs G.A.D., Stockli T., Méténier K., Bonnamy S., Béguin F., Burnham N.A., and Forró L. Elastic modulus of ordered and disordered multiwalled carbon nanotubes. *Advanced Materials*, 11(2):161–165, 1999.

Sandler J., Werner P., Shaffer M.S.P., Demchuk V., AltstÃd'dt V., and Windle A.H. Carbon-nanofibre-reinforced poly(ether ether ketone) composites. *Composites Part A: Applied Science and Manufacturing*, 33(8):1033–1039, 2002.

Thostenson E.T. and Chou T. On the elastic properties of carbon nanotube-based composites: modelling and characterization. *J. Phys. D: Appl. Phys.*, 36:573–582, 2003.

Xie S., Li W., Pan Z., Chang B., and Sun L. Mechanical and physical properties on carbon nanotube. *Journal of Physics and Chemistry of Solids*, 61(7):1153–1158, 2000.

Yu M.F., Lourie O., Dyer M.J., Moloni K., Kelly T.F., and Ruoff R.S. Strength and breaking mechanism of multiwalled carbon nanotubes under tensile load. *Science*, 287(5453):637–640, 2000.

Zhou X., Shin E., Wang K.W., and Bakis C.E. Interfacial damping characteristics of carbon nanotube-based composites. *Composites Science and Technology*, 64:2425–2437, 2004.